

ENHANCEMENT OF THE SIDE EMISSION EFFICIENCY OF COMMERCIAL PMMA OPTICAL FIBRES IN THE UV-A AND VISIBLE BLUE SPECTRUM FOR PHOTOCURING OF EPOXY RESINS

Ammar D. Alobaidani ^{a+}, David Furniss ^a, Andreas Endruweit ^a, Michael S. Johnson ^a, Trevor Benson ^b and Angela B. Seddon ^a

^a School of Mechanical, Materials and Manufacturing Engineering, University of Nottingham, University Park, Nottingham, NG7 2RD, U.K.

^b School of Electrical and Electronic Engineering, University of Nottingham, University Park, Nottingham, NG7 2RD, U.K.

⁺ eaxad@nottingham.ac.uk

ABSTRACT

Transmission measurements of commercial PMMA optical fibres at different lengths indicated that, due to discrete defects, the attenuation is non-uniform along the fibres. Because of these defects, even untreated fibres show a certain degree of side emission. Transmission losses due to side emission at fibre bends increase with increasing bending angle (or number of full loops), increasing fibre diameter and decreasing bend radius. Geometry modification of a fibre (bends with defined radii) allows a defined level of side emission to be achieved. Mechanical treatment of the fibres by application of micro-cuts and embedding scattering silica particles results in side emission of most of the power launched into the fibres. Fibres treated by embedding silica particles and geometry modification gave the best results in terms of side emission intensity. Embedding a fibre of this type in an epoxy resin system allowed photocuring of the resin to be achieved.

1. INTRODUCTION

Photocuring of polymers and polymer composites by means of irradiation in the ultraviolet (UV) spectrum shows several potential advantages compared to thermal curing. The cycle time is significantly reduced (minutes rather than hours) and, as no heating is required, the energy consumption in UV curing is typically lower and the tool design is less complex. Since the curing process normally starts from the component surface, liquid resin is encapsulated below the surface, and the emission of volatile substances into the environment can be significantly lowered. However, conventional UV curing methods can only be applied as long as the component can be directly irradiated and, due to the absorption of radiation, the material thickness for efficient application of UV curing is limited. The motivation for studying the feasibility of photocuring processes using side emission optical fibres embedded in the component, is the potential to achieve compatibility with economical closed mould processes, such as Resin Transfer Moulding, to allow curing of thick-sectioned components, and to cure adhesives in bond lines between opaque material sheets.

In optical fibres for telecommunication and data transfer applications, light is transmitted with, ideally, minimum loss and emitted only from the end face. Side emission optical fibres, on the other hand, are designed as linear light sources for illumination and decoration purposes. Side light emission can be achieved by various means. In a recent study [1], various types of commercial side emission optical fibres were characterised. They were found either to consist of a silica core with a cladding containing scattering particles (Al_2O_3 or ZnO), or of a core of poly(methyl methacrylate) (PMMA) and a poly(vinylidene fluoride) cladding with micro-perforations.

The challenge in photocuring of polymers is that UV light, which in general is subject to stronger attenuation while transmitted through fibres than visible light, is utilised, and that the amount of energy transferred by the light is critical for initiation of the photoreactions [2-4]. The total rate of energy absorption [5] by the photoinitiator to produce reactive species, which determines the efficiency of the curing process, is given by

$$e = \int_0^{\infty} \kappa_{\lambda} E_{\lambda} d\lambda \quad , \quad (1)$$

where λ is the wavelength, κ_{λ} is the response spectrum of the resin system and E_{λ} is the emission spectrum of the irradiating light source. This implies that the maximum curing efficiency can be achieved if E_{λ} and κ_{λ} are well matched. For illustration, the absorption spectra of two epoxy resin systems are compared with the emission spectrum of a side emission optical fibre (Figure 1). The figure shows that the response spectrum of a resin system can be enhanced by addition of anthracene photosensitiser (curve B), as discussed by Cho et al. [6]. Due to the overlap of curve B with one of the peaks in the emission spectrum of the fibre (curve C), resin specimens could eventually be cured, although the intensity of light emitted from the fibre is low.

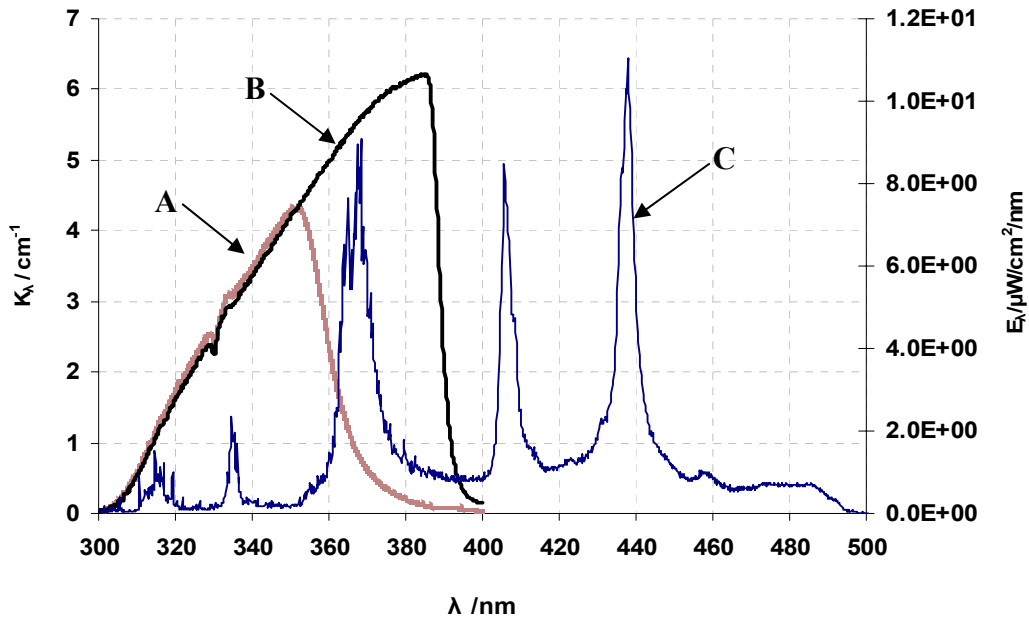


Figure 1: (A) Response spectrum κ_{λ} of epoxy resin system 1 (cycloaliphatic epoxy, triarylsulfonium salt photoinitiator, oxetane diluent); (B) response spectrum κ_{λ} of epoxy resin system 2 (resin 1 with anthracene photosensitiser); (C) side emission spectrum E_{λ} of a commercial PMMA optical fibre (1 mm diameter, side treated with micro-perforations), recorded at a distance $x_0 = 13.65$ cm from the launch face and a radial distance $r = 2$ mm from the fibre axis.

The PMMA core fibres exhibit generally a higher intensity of side light emission, in particular in UV, and thus prove more suitable for photocuring applications than typical commercial silica core fibres [1]. However, in order to improve the efficiency of the photocuring process, further enhancement of the emitted light intensity (at a given

intensity of the light launched into the PMMA core of the fibres) is desirable. In this context, this study aims at the characterisation of the transmission of PMMA optical fibres and the enhancement of their side emission efficiency in the spectral range from UV-A to visible blue.

2. MATERIALS AND METHODS

For the experiments carried out in this study, a BlueWave 200 (Dymax Corp.) light source was used with a nominal power of 200 W, designed to deliver a light beam for spot curing applications. This light source was equipped with a mercury (“H”) bulb with major emission peaks at wavelengths of 365 nm, 406 nm and 440 nm (see Figure 1). The effective flux density was approximately 40 W/cm² over the spectral range from 280 nm to 450 nm.

The different commercial PMMA optical fibres used in this study are described in Table 1. All fibres were fitted in-house with aluminum connectors at the launch ends. After fitting the connectors, both end faces of each fibre were polished to reduce refraction and scattering. The fibres were connected to the light source via an ice-filled cooling device, made from aluminum for efficient heat conduction. This allowed centring of the fibres relative to the emitted light beam and protected the launch faces from thermal degradation due to heating induced by the high-power irradiation, which could potentially reduce the intensity of light launched into the fibre.

The study of the PMMA optical fibres was based on three sets of experiments: determination of the fibre attenuation (intrinsic and extrinsic), quantification of side emission at fibre bends, and modification of the fibres to improve the side emission efficiency. The power transmission through the fibres was measured using a Molectron analogue power meter (PM500A), and the side emission was characterised using an Ocean Optics USB4000 spectrometer.

Table 1: Characterisation of the different commercial PMMA optical fibres used in this study.

Fibre	Core material	Cladding material	Fibre diameter / μm	Core diameter / μm	Cladding thickness / μm	Fibre treatment
1	Poly(methyl methacrylate)	Poly(vinylidene fluoride)	500	486	7	Untreated
2			750	738	6	Untreated
3			1000	980	10	Untreated
4			1551	1494	29	Untreated
5			1551	1494	29	Surface micro-perforation

3. RESULTS AND DISCUSSION

3.1 Fibre transmission

The attenuation of PMMA optical fibres was determined in cut-back tests. The total transmitted power was measured at the fibre end face, starting at a fibre length of 1.1 m, which was then reduced in steps of 10 cm. This technique allowed the attenuation per 10 cm long fibre segment to be determined and localised defects, which could have caused transmission losses, to be identified. The results plotted in Figure 2 show that the attenuation of 10 cm long fibre segments varied randomly along the fibres. At a

length of 1 meter, different specimens of fibre 4 transmitted between 525 mW and 600 mW. However, for longer fibres, the transmission readings are expected to converge. Figure 3 shows the intensity of side emission of an untreated fibre. Relating Figure 3 with Figure 2 suggests that, as discussed elsewhere [1], the power loss in transmission due to localised defects is converted to side emission.

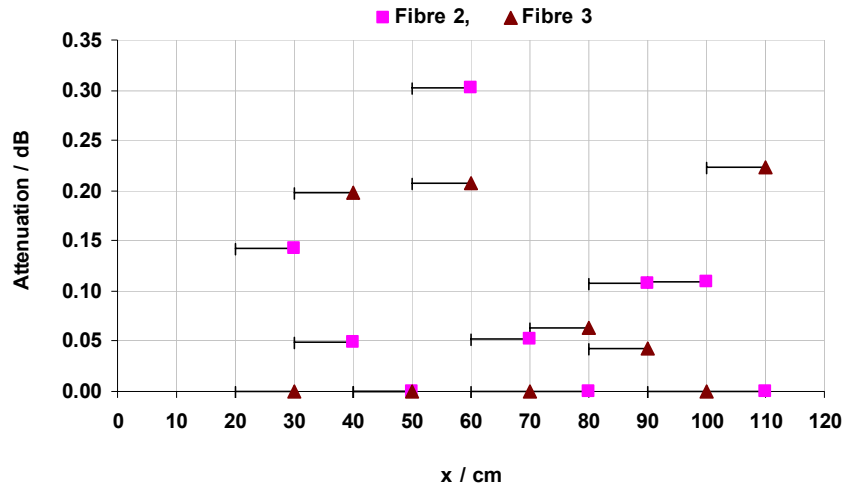


Figure 2: Attenuation of 10 cm long fibre segments as a function of the position x along the fibre for the examples of fibre 2 and fibre 3 (see Table 1).

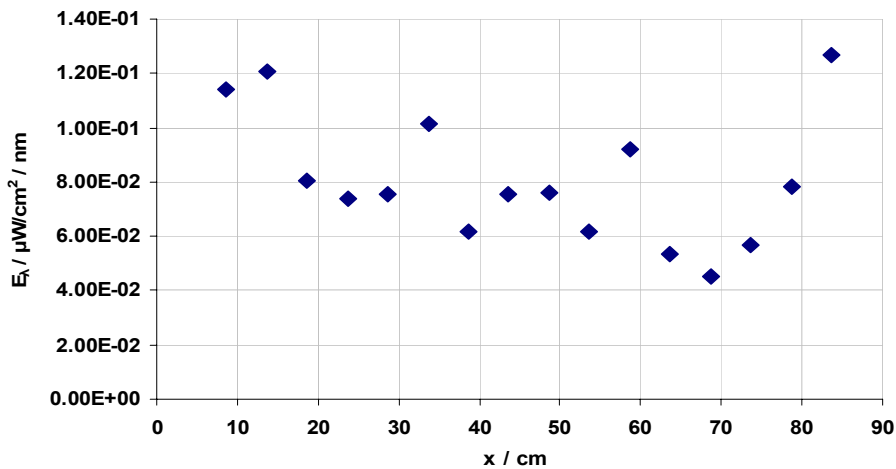


Figure 3: Irradiance E_λ at $\lambda = 365$ nm as a function of the position x along fibre 2, measured at radial distance $r = 2$ mm from the fibre axis.

3.2 Bend losses

The loss in transmitted power, which corresponded to the total power emitted from the fibres at bends, was studied for optical fibres at different fibre diameters, bend radii, and numbers of fibre loops (360° bends). The total transmission was measured at the fibre end face for bend radii of 25 mm, 12.5 mm and 4 mm. For each bend radius, the experiment was repeated at one, two and three full loops. The attenuation as a function of the number of loops is plotted in Figure 4 for the examples of fibre 1, fibre 3 and fibre 4. For all fibres, the surrounding medium was air. For an additional experiment, fibre 3 was immersed in a cycloaliphatic epoxy resin. Since the refractive index of air is

lower than that of the fibre cladding ($n_{\text{cladd}} = 1.42$ [1]), and the refractive index of the epoxy resin is higher ($n_{\text{epoxy}} = 1.45$ [10]), this change of experimental conditions was expected to affect light guiding in the fibre.

Fibre 1 and fibre 4 showed no change in attenuation at a loop diameter of 50 mm (Figures 4A and 4C). At a loop diameter of 25 mm, the attenuation of fibre 1 did not vary with increasing number of loops, while the attenuation of fibre 4 increased until it reached 2.2 dB in the third loop. Fibre 3 shows increasing attenuation at loop diameters of 50 mm and 25 mm. All fibres show a significant increase in attenuation at the smaller loop diameter of 8 mm. These results are in agreement with the observations documented by Durana et al. [11]. Generally, the increase in attenuation with increasing number of loops is the more significant, the greater the fibre diameter. Fibre 3 showed increased power loss, i.e. increased side emission, when immersed in a medium with higher refractive index than the cladding.

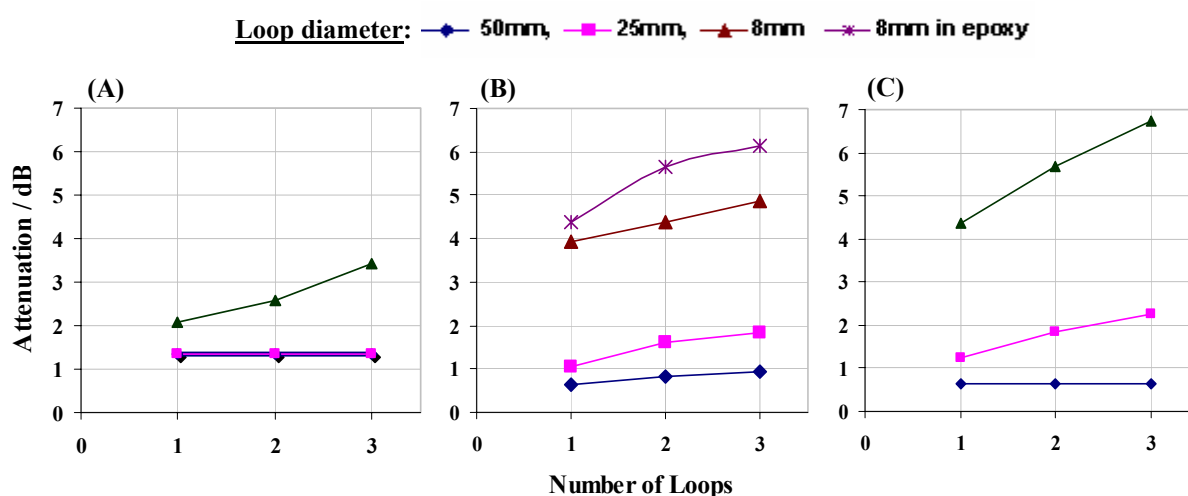


Figure 4: Attenuation as a function of the number of full turns of 1 metre long fibres, parameter loop diameter; (A) fibre 1, (B) fibre 3, (C) fibre 4 (Table 1); for fibre 3, the effect of immersion in cycloaliphatic epoxy resin is also illustrated.

3.3 Side emission enhancement

3.3.1 Geometrical modification

The geometry of PMMA optical fibres was modified permanently by heat treatment. The fibres were shaped on an in-house made aluminum tool, which allowed adjusting of the bend radii. The tool with the fibres wound on it was then placed in an oven for fifteen minutes at a temperature of 70 °C (in ambient air). The original length of all specimens was 245 mm. Different geometrical modifications, schematically illustrated in Figure 5, were tested regarding the total power transmission of the treated fibres. The bending radii were selected based on the results discussed in section 3.2.

The power losses in side emission are compared in Table 2 for the different treated fibres. The results indicate that, at a given fibre diameter, the side emission increased with decreasing bend radius. At a given bend radius, the side emission increased with increasing fibre diameter. Due to the process of geometrical modification, sharp bends (reduced bend radius) may have occurred near the fibre ends (Figure 5B and Table 2), possibly resulting in increased local emission. These sharp bends should be avoided to achieve more uniform side emission. For fibres modified by bends with identical radii, the side emission decreased significantly along the fibre. To achieve more uniform

emission, fibres were modified by multiple bends of decreasing radii, i.e. increasing side emission, along the fibre (Figure 5C).

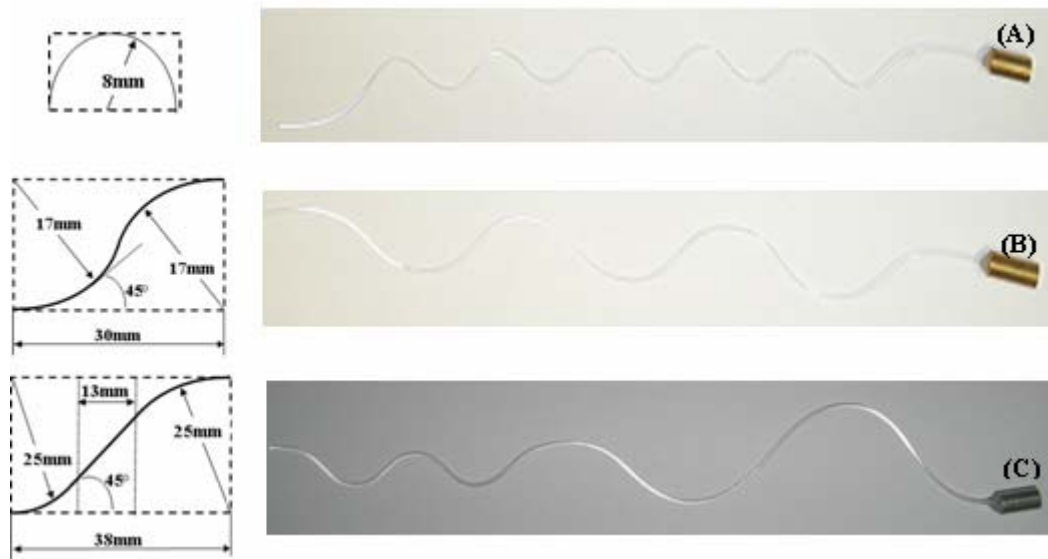


Figure 5: Examples of geometrical modification (details of the bend geometries shown on the left); (A) ten bends, 8 mm radius, (B) twelve bends, 17 mm radius, (C) ten bends, different radii, three bends similar to example A, two bends similar to example B, five bends with dimensions as shown on the left.

Table 2: Transmission through fibres exhibiting different geometrical modifications. The original length of all fibres before geometrical modifications was 245 mm.

Fibre	Fibre modification	Total power transmission of fibre		Loss in transmitted power
		untreated / mW	treated / mW	
2	as in Figure 5B (sharp bend)	155	130	16.1 %
	as in Figure 5B (no sharp bend)		140	9.7 %
	as in Figure 5A		70	54.8 %
	as in Figure 5C		110	29.0 %
4	as in Figure 5B (sharp bend)	525	120	77.1 %
	as in Figure 5B (no sharp bend)		270	48.6 %
	as in Figure 5A		15	97.1 %
	as in Figure 5C		150	71.4 %

3.3.2 Mechanical treatment

In the commercial PMMA side emitting optical fibre (fibre 5), side emission was achieved by micro-perforation of the cladding. These micro-holes were found to vary in size and to be distributed non-uniformly (Figure 6). This irregularity of the perforation results in strong fluctuations of the side emission [1].

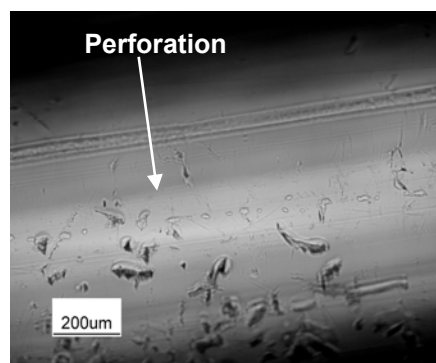


Figure 6: Optical reflection microscopic image of fibre 5 (Table 1), showing irregular surface perforations.

To achieve more consistent side emission along the fibre, other techniques can be used. Sillyman et al. [12] controlled the side emission by creating notches in the fibre cladding. Varying the distances between the notches along the fibre allowed uniform emission to be obtained. Zarian et al. [13] suggested that uniform high rates of side emission can be achieved by applying micro-cuts on the fibre core. Joseph et al. [14] and Yokogawa et al. [15] demonstrated the use of scattering particles, either in the fibre core or cladding. In addition, launching light at both ends of the fibre further improves side emission uniformity as demonstrated by Spigulis et al. [16].

Here, the untreated PMMA optical fibres (Table 1) were modified by micro-cutting and embedding of silica particles to study the possibility of achieving maximum side emission. Micro-cuts with depths less than 100 μm at 1 cm intervals along the fibre were applied to the poly(vinylidene fluoride) cladding using a sharp object. Silica particles of sizes ranging from $\sim 2 \mu\text{m}$ to 70 μm (Figure 7) were mechanically embedded in the cladding. Silica was selected because of its high UV transmission [17]. The depth of micro-cuts and the sizes of the silica particles were selected so that the treatments affected both the cladding and the core of the fibres. The densities of the micro-cuts and of the silica particles were increased progressively to increase side emission. Both treatments were studied individually and in combination. The length of all treated fibre specimens was 245 mm.

Measurement of the total power transmission indicated that the side emission efficiency of the fibres increased with increasing number of micro-cuts in the cladding. Relative to the total power transmitted through an untreated fibre, up to 60 % side emission was achieved (85 micro-cuts along the fibre). Further increase of the number of micro-cuts reduced the mechanical integrity of the fibre. Embedding silica particles in the cladding of the fibre (particles evenly distributed along the fibre, total mass 3×10^{-3} g) resulted in side emission of 81 % of the total power. A combination of micro-cuts and silica particle treatment (Figure 8) resulted in 94.5 % side emission. The micro-cuts were applied before the silica particles were embedded, allowing silica particles to be embedded both in the micro-cuts and the undamaged poly(vinylidene fluoride) cladding (Figure 8).

Further enhancement of the side emission efficiency can be achieved by combining mechanical treatment of the fibre with geometrical modification. Reshaping fibre 3 (245 mm long) to twelve bends with 17 mm radius resulted in side emission of 31 %. The same fibre showed 96 % side emission when treated by combining silica mechanical treatment with geometrical modification, as shown in Figure 9.

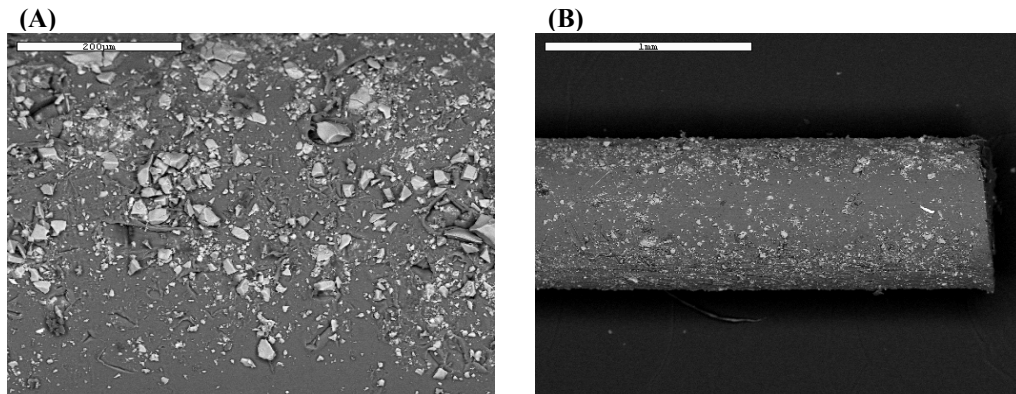


Figure 7: Microscopic images of fibre 2 (750 µm diameter) with embedded silica particles; (A) different sizes of silica particles; (B) distribution of silica particles across fibre surface.

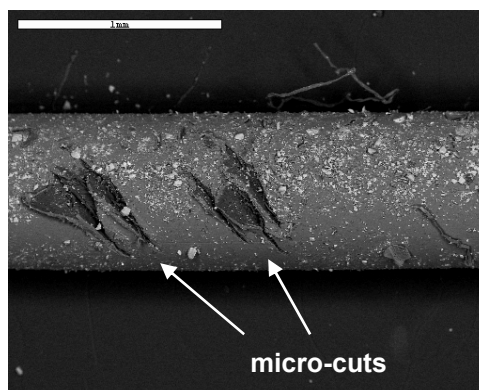


Figure 8: Microscopic image of fibre 2, treated with silica particles and micro-cuts.



Figure 9: Fibre 3, treated with silica particles, twelve bends with 17 mm radius; bright spots indicate emission at scattering particles.

4. CONCLUSIONS

Photocuring of epoxy resins using embedded side emission optical fibres has potential applications in closed mould processes, such as Resin Transfer Moulding, for curing of thick-sectioned components, and for curing adhesives in bond lines between opaque material sheets. For this reason, the transmission of PMMA optical fibres was studied,

and their side emission efficiency in the spectral range from UV-A to visible blue was enhanced.

Transmission measurements for PMMA optical fibres at different lengths indicated that, due to discrete defects, the attenuation is non-uniform along the fibres. Due to these effects, even untreated fibres show a certain degree of side emission.

Transmission losses due to side emission at fibre bends increase with increasing bending angle (or number of full loops), increasing fibre diameter and decreasing bend radius. Geometrical modification of a fibre (bends with defined radii) allows a defined level of side emission to be achieved.

Mechanical treatment of the fibres by application of micro-cuts and embedding scattering silica particles resulted in side emission of most of the power launched into the fibres.

Fibres treated by embedding silica particles and geometry modification gave the best results in terms of side emission intensity. A side emission of 96 % of the total power launched into the fibre was observed. Embedding a fibre of this type in an epoxy resin system allowed photocuring of the resin to be achieved.

REFERENCES

- 1- Endruweit, A., Alobaidani, A.D., Furniss, D., Seddon, A., Benson, T., Johnson, M.S., Long, A., "Spectroscopic experiments regarding the efficiency of side emission optical fibres in the UV-A and visible blue spectrum", *Optics and Lasers in Engineering*, 2008; 46: 97-105.
- 2- Decker, C., "Photoinitiated Crosslinking Polymerization", *Progress in Polymer Science*, 1996; 21: 593-650.
- 3- Crivello, J.V., "Photoinitiated Cationic Polymerization", *Annual Review of Material Science*, 1983; 13: 173-190.
- 4- Fouassier, J.P., Ruhlmann, D., Graff, B., Wieder, F., "New insights in photosensitizers-photoinitiators interaction", *Progress in Organic Coating*, 1995; 25: 169-202.
- 5- Cassano, A.E., Martin, C.A., Brandi, R.J., Alfano, O.M., "Photoreactor analysis and design: Fundamentals and applications", *Industrial & Engineering Chemistry Research*, 1995; 34: 21-55.
- 6- Cho, J.D., Kim, E.O., Kim, H.K., Hong, J.W., "An investigation of the surface properties and curing behaviour of photocurable cationic films photosensitized by anthracene", *Polymer Testing*, 2002; 21: 781-791.
- 7- Weinert, A. (editor), "Plastic optical fibers: principles, components, installations". Erlangen: Publicis MCD Verlag; 1999.
- 8- Baumer, S. (editor), "Handbook of plastic optics". Eindhoven: Wiley-VCH; 2005.
- 9- Zubia, J., Arrue, J., "Plastic optical fibers: an introduction to their technological processes and applications", *Optical Fiber Technology*, 2001; 7: 101-140.
- 10- Yonemura, M., Kawasaki, A., Kato, S., Kagami, M., "Polymer waveguide module for visible wavelength division multiplexing plastic optical fiber communication", *Optics Letters*, 2005; 30: 2206-2208.
- 11- Durana, G., Zubia, J., Arrue, J., Aldabaldetrek, G., Javier, M., "Dependence of bending losses on cladding thickness in plastic optical fibers", *Applied Optics*, 2003; 42: 997-1002.
- 12- Sillyman, S., Li, K., Inatsugu, S., "Source numerical aperture control for efficient light emission from notched, side-lighting fiber optics", *Proceedings of SPIE*, 2004; 5529: 70-78.

- 13- Zarian, J.R., Robbins, J.A., Sitar, D., Holme, J.A., "Side lighting optical conduit". United States Patent 5987199, 1999.
- 14- Joseph, E., Smith, G., "Side scattering light guide", United States patent. pub. No. US 2006/0140562 A1, 2006.
- 15- Yokogawa, H., Yokoyama, M., Sonoda, K., Kousaka, K., "Side face illuminating optical fiber", United States Patent 6154595, 2000.
- 16- Spigulis, J., Pfafrods, D., Stafekis, M., Jelinska-platace, W., "The 'glowing' optical fibre designs and parameters", *Proceedings of SPIE*, 1996; 2967: 231-236.
- 17- Zou, X., Itoh, K., Toratani, H., "Transmission loss characteristics of fluorophosphate optical fibers in the ultraviolet to visible wavelength region", *Journal of Non-Crystalline Solids*, 1997; 215: 11-20.